Nature-Inspired Multifunctional Ligands: Focusing on Amyloid-Based Molecular Mechanisms of Alzheimer's Disease

(Article begins on next page)

19 April 2024

Nature-inspired multifunctional approach: focusing on amyloid-based molecular mechanisms of Alzheimer's disease

Elena Simoni,[a] Melania M. Serafini,[b] Manuela Bartolini,[a] Roberta Caporaso,[a] Antonella Pinto,[b] Daniela Necchi,[b] Jessica Fiori,[a] Vincenza Andrisano,[c] Anna Minarini,[a] Cristina Lanni,*[b] and Michela Rosini*[a]

Abstract: The amyloidogenic pathway is a prominent feature of Alzheimer's disease (AD). However, growing evidence suggests that a linear disease model based on amyloid-β peptide (Aβ) alone is not likely to be realistic, thus calling for further investigations on the other actors involved in the play. The pro-oxidant environment induced by Aβ in AD pathology is well established, and a correlation between Aβ, oxidative stress and p53 conformational changes has been suggested. Here, we applied the multifunctional approach to identify the nature-inspired ligands **1-3**, whose pharmacological profile was strategically tuned by the hydroxyl substituents on the aromatic moiety. Indeed, only catechol **3** inhibited Aβ fibrilization, by acting at the early stage of amyloid aggregation. Conversely, albeit to a different extent, all compounds were able to reduce ROS formation in SH-SY5Y neuroblastoma cells. In the same cell line, **1-3** prevented alterations in p53 conformation and activity mediated by soluble sublethal concentrations of Aβ. This may support an involvement of oxidative stress in Aβ function, with p53 emerging as a potential mediator of their functional interplay.

Introduction

Alzheimer's disease (AD) is a progressive neurodegenerative disorder, with a complex interplay of genetic and biochemical factors contributing to the pathological decline. Progression of the disease involves misfolding and aggregation of amyloid-β peptide (Aβ) from soluble non toxic monomers into insoluble fibrils. The most toxic form of Aβ is believed to be soluble oligomers, which are potent mediators of the synaptotoxicity.[1] In AD drug development, programs based on the Aβ cascade hypothesis have dominated research for the past twenty years, and still play a major role in pharmaceutical product pipelines.

[a]   Dr. E. Simoni, Prof. Dr. M. Bartolini, R. Caporaso, Dr. J. Fiori, Prof.
        Dr. A. Minarini and Prof. Dr. M. Rosini*
        Department of Pharmacy and Biotechnology
        Alma Mater Studiorum-University of Bologna
        Via Belmeloro 6, 40126 Bologna, Italy
        E-mail: michela.rosini@unibo.it

[b]   M. M. Serafini, A. Pinto, Dr. D. Necchi, Dr. C. Lanni*
        Department of Drug Sciences (Pharmacology Section)
        University of Pavia
        V.le Taramelli 14, 27100 Pavia, Italy
        E-mail: cristina.lanni@unipv.it

[c]   Prof. Dr. V. Andrisano
        Department for Life Quality Studies
        Alma Mater Studiorum-University of Bologna
        Corso d'Augusto 237, 47921 Rimini, Italy

However, Aβ-centric approaches have not yet resulted in clinically effective drugs. This has raised a degree of skepticism, which has in turn led to review the science underpinning the Aβ model.[2] Besides the consolidated evidence that Aβ might trigger the disease process, intertwined correlations between Aβ and the other main players of the disease have been identified.[3] This has prompted researchers to develop multifunctional anti-amyloid agents[4] that, by acting simultaneously on several AD targets than the amyloidogenic pathway alone, are intended to trigger a synergistic response, with superior efficacy and safety profile.[5] Further, we think that molecules endowed with a multifaceted pharmacology have a great potential in exploring Aβ partnership with other crucial AD features. A deeper comprehension of amyloid-based disease mechanisms might offer the chance for repositioning Aβ in the disease network, being of help in bridging the gap between basic and translational research. In particular, the etiopathogenic loop generated by Aβ and oxidative stress offers a new key for reading Aβ causative role.[6] Oxidative stress is known to trigger the amyloidogenic pathway and promote Aβ toxicity.[7] On the other hand, several lines of evidence indicate that Aβ exacerbates oxidative stress, with other cellular pathways emerging as determining mediators of this vicious cycle.[8] In this respect, regulation of p53 conformation and function may represent a crucial feature of this puzzling scenario.

p53 is a tumor suppressor protein primarily involved in cancer biology. However, recent observations have showed that p53 may also play a central role in aging and in neurodegenerative disorders.[9] Conformational changes and functional alterations of p53 have been found in patients with AD.[10] Unfolded p53 is not able to exert its pro-apoptotic activity in AD cells, leading to aberrant cell cycle progression,[11] and to the accumulation of aging-associated abnormalities. p53 is an intrinsically unstable protein, whose conformation and DNA binding domain can be modulated by metal chelators and redox status.[12] In particular, an alteration in oxidative homeostasis, resulting in a subtoxic and chronic ROS exposure, impairs wild-type p53 tertiary structure, inducing a switch toward the not functional unfolded form of p53.[13] The alteration of the physiological functions of p53 can also result from the exposure to soluble non toxic Aβ, and has been shown to be related to the ability of Aβ to interfere with two key proteins, i.e. zyxin and the homeodomain-interacting protein kinase 2 (HIPK2).[14] Zyxin is an adaptor protein identified as a regulator of HIPK2-p53 signaling in response to DNA damage.[15] HIPK2 activity is in turn fundamental in maintaining wild-type p53 function, controlling the destiny of cells when exposed to DNA damaging agents. In particular, soluble Aβ peptides downregulate zyxin expression, which is fundamental in maintaining HIPK2 stability and in turn p53 activity.[14b] This Aβ-mediated downregulation may be responsible for early pathological changes that precede the amyloidogenic pathway in the neurodegenerative cascade.
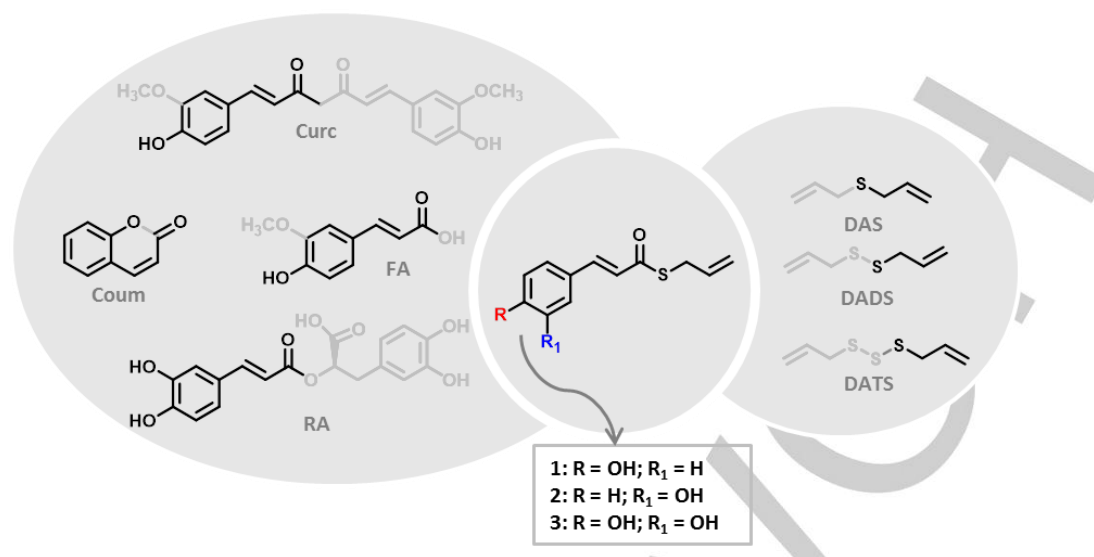
Figure 1. Design strategy for compounds **1-3**. Left side: Curc (curcumin), Coum (coumarin), FA (ferulic acid), RA (rosmarinic acid). Right side: DAS (diallyl sulfide), DADS (diallyl disulfide), DATS (diallyl trisulfide).

Therefore, the induction of the unfolded state of p53, by leading to the accumulation of dysfunctional neurons in the CNS, is emerging as a novel amyloid-based mechanism of AD pathogenesis.

As a part of our ongoing work aimed at deepening insight the cross-talk between Aβ functions and oxidative stress in AD, we envisioned nature as a structural "muse". Natural products offer a great chemical diversity,[16] and have already proven to be a rich source of therapeutics. Polyphenols are widely diffused in nature. They have been shown to modulate several AD pathways, including oxidative injuries and Aβ aggregation.[17] Interestingly, many of them present a hydroxy-cinnamoyl function as a recurring motif. On the other hand, diallyl sulfides are garlic-derived organosulfur compounds carrying allyl mercaptan moieties. They counteract oxidative stress through antioxidant enzyme expression.[18] Herein, we combined these privileged molecular fragments in new chemical entities, affording hybrids **1-3** (Figure 1).

Synthesized compounds were first tested *in vitro* to assess their antiaggregating properties towards Aβ$_{42}$, the most amylodogenic isoform of Aβ. They were then assayed in neuroblastoma cells to explore their ability to counteract oxidative stress and to exert neuroprotective effect against Aβ$_{42}$-induced toxicity.

The efficacy of **1-3** in modulating Aβ-induced conformational state alteration of p53 protein was also investigated. Curcumin was herein the reference compound. Based on its pleiotropic nature, curcumin is a consolidated prototype for AD studies, and it has already provided an outstanding platform for numerous biologically active ligands.[19]

Results and Discussion

Synthetic chemistry. Syntheses of **1-3** were carried out in a linear fashion as depicted in Scheme 1. *tert*-Butyldimethylsilyl (TBDMS)-protection of the alcohol followed by coupling reaction
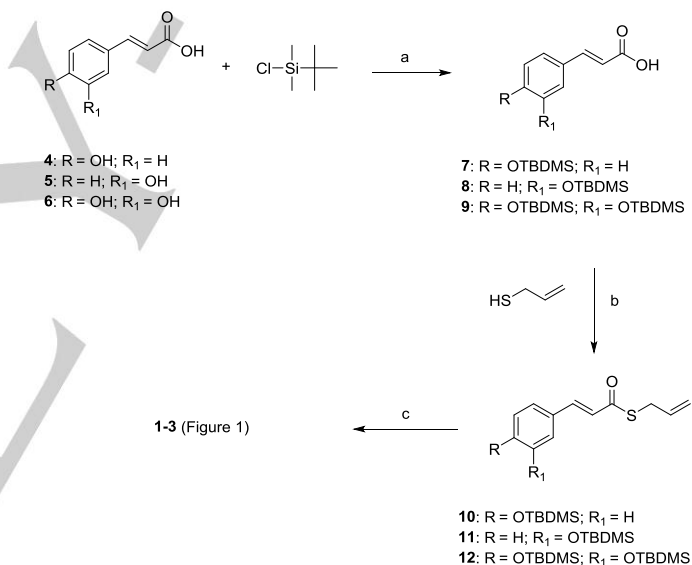
Scheme 1. Reaction conditions: (a) DMF, imidazole, N$_2$, o/n, rt; (b) DCC, DMAP, CH$_2$Cl$_2$, N$_2$, o/n, 0°C-rt; (c) TBAF, THF, N$_2$, 30', rt.

with DCC in presence of DMAP gave the intermediates **10-12**. Finally, treatment of **10-12** with tetrabutylammonium fluoride (TBAF) effected desilylation to give the final compounds **1-3**.

Synthesized molecules have been characterized by NMR spectroscopy and ESI mass spectrometry. ^{1}HNMR spectra show that all compounds have an *E* configuration as indicated by the large spin coupling constants (around 16 Hz) of α-H and β-H on double bonds.

Inhibition of Aβ$_{42}$ self-aggregation (ThT-based assay). We have fostered the development of nature-inspired multifunctional ligands as an attractive opportunity to gain insight the cross-talk between oxidative damage and Aβ pathways. Therefore, synthesized compounds were first tested to evaluate their possible anti-aggregating properties by means of a thioflavin T

(ThT)-based fluorometric assay. ThT dye shows a characteristic red shift in the excitation/emission spectrum and an increase in the quantum yield upon binding to fibrillar β-sheet structures.[20] The ThT-based assay is commonly used to monitor Aβ fibrillization and its inhibition.

The evaluation of **1-3** clearly highlights a strong influence of the aryl decoration on the ability to prevent the $A\beta_{42}$ self-assembly process. Interestingly, the catechol moiety (compound **3**) turned out to be essential for activity. **3**, at 1/1 ratio with $A\beta_{42}$ almost completely inhibited $A\beta_{42}$ self-aggregation (% inhibition > 90%), resulting even more effective than curcumin (% inhibition = 73.7%). Noteworthy, in the same experimental conditions, a complete loss of the anti-aggregating efficacy was observed for **1** and **2**, lacking the *m*- or *p*-hydroxyl function, respectively (Figure 2).
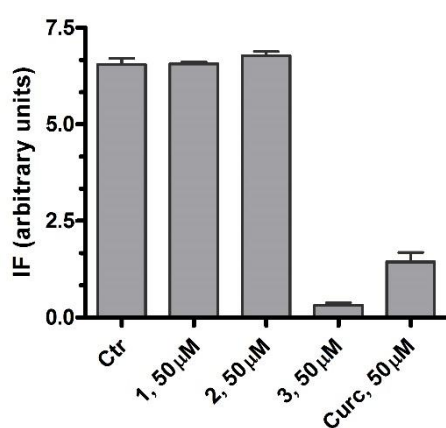

Figure 2. Inhibition $A\beta_{42}$ aggregation by **1-3** or Curc as determined by a ThT-based assay. ThT-related fluorescence intensity of $A\beta_{42}$ (50 µM) samples after a 24h-incubation period in the absence (Crtl) or in the presence of the tested compound (50 µM). The values are the mean of two independent measurements each performed in duplicate.

This striking result points to the catechol moiety as a key recognition fragment in amyloid binding. The inhibitory effect exerted by **3** resulted to be concentration-dependent, giving an IC_{50} value of 12.5 ± 0.9 µM. Based on this value, **3** can be considered a good inhibitor of $A\beta_{42}$ self-aggregation, owning an inhibitory potency similar to the well known multipotent compound bis(7)tacrine (IC_{50} = 8.4 ± 1.4 µM)[21] and derivative D737 ($IC_{50} \sim$ 10 µM),[22] and being only five times less potent than the flavonoid myricetin (2.60 ± 0.33 µM).[23]

To explore the possibility of tuning the anti-aggregating profile of **3**, a detailed structure-activity relationship study is in progress and will be published in due course.

Inhibition of $A\beta_{42}$ self-aggregation (MS assay). Motivated by the promising results, we sought to gain a deeper understanding of **3**'s mode of action at a molecular level using an orthogonal method, i.e., electrospray ionization-ion trap-mass spectrometry (ESI-IT-MS) in flow injection mode, which allows to detect and quantitate the monomeric form of $A\beta_{42}$.[23] Amyloid aggregation was monitored by evaluating the Aβ monomer decrease after

24h incubation in the presence and absence of the tested inhibitor, using reserpine as internal standard (IS). In the used experimental conditions, in the absence of any inhibitor, a progressive decrease in the monomer content, expressed as the sum of the native ($A\beta_{42}$ Native) and oxidized form ($A\beta_{42}$ Ox) of $A\beta_{42}$, is observed within 24h, due to inclusion of Aβ monomers into growing stable oligomers.[24] In agreement with this trend, when $A\beta_{42}$ was incubated alone, a dramatic decrease (83%) in monomer content was observed after 24h incubation (Figure 3).

Conversely, when treating $A\beta_{42}$ with **3** in a peptide/inhibitor ratio of 1/1, after 24h incubation a high monomer content was detected, meaning that **3** strongly inhibited monomer inclusion into growing amyloid oligomers (Figure 3). Indeed, the residual percentage of $A\beta_{42}$ monomer at 24h was only 17 % in the absence of any inhibitor and 78 %, in the presence of **3**. Curcumin, tested in the same conditions, resulted to be a much weaker inhibitor of the early phase $A\beta_{42}$ aggregation (residual percentage of monomer after 24h incubation = 36 %).

These results, other than confirming the antiaggregating activity resulting from the ThT-based assay, also showed that **3** was able to strongly retard the Aβ overall assembly process by acting at monomer level in the early stage of the amyloid aggregation and strongly preventing the formation of stable soluble oligomers. This is of utmost importance because of the cytotoxic effects exerted by soluble aggregation intermediates.[25] The overall inhibition percentage was 74.5 ± 6.5%, in agreement with data obtained with the ThT fluorometric assay. On the other hand, curcumin showed a % inhibition of 22 ± 7.6%.

Previous studies performed on the natural polyphenol myricetin showed pro-oxidant properties toward $A\beta_{42}$ peptide.[24] These properties can be explained by the well-accepted attitude of polyphenols to act as either antioxidant or pro-oxidant agents.[26] The oxidized form of $A\beta_{42}$ ($A\beta_{42}$ Ox) was shown to be less prone to aggregate than the native one ($A\beta_{42}$ Native), thus accounting for a slower aggregation rate.[27] With these concepts in mind, we sought to verify whether **3**, bearing a catechol moiety, could partially exert its inhibitory activity through an oxidation-based mechanism. Based on the different molecular weight, both the native and oxidized forms of $A\beta_{42}$ can be detected by MS analysis. Worth mentioning, a small percentage of $A\beta_{42}$ Ox is always present in $A\beta_{42}$ commercial samples (around 15%, detectable at t0), and, in agreement with the $A\beta_{42}$ Ox lower inclination to aggregate, the initial content of the oxidized Aβ species just slightly decreases after 24h incubation (Figure 3).[24]
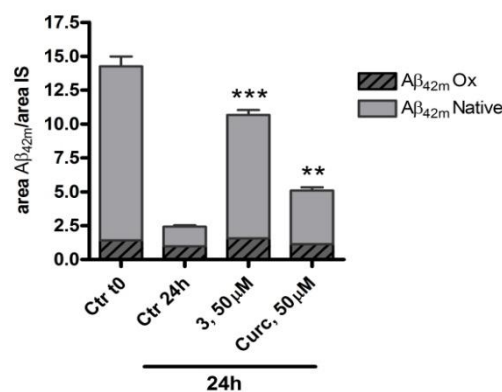
Figure 3. Inhibition of $A\beta_{42}$ aggregation by **3** and curcumin (Curc) as determined by ESI-IT-MS method. The total $A\beta_{42}$ monomer ($A\beta_{42m}$) content in the absence (Ctrl) and in the presence of inhibitor is displayed as the sum of the native ($A\beta_{42}$ Native) and oxidized form ($A\beta_{42}$ Ox) of $A\beta_{42}$. IS stands for internal standard (reserpine). ** $p < 0.01$, *** $p < 0.001$ versus Crtl 24h; Dunnett's Multiple Comparison Test.

When treating $A\beta_{42}$ samples with **3** in a peptide/inhibitor ratio of 1/1, only a slightly increase of the oxidized species at 24h with respect to the initial content was observed, thus excluding a significant oxidation-mediated mode of inhibition (Figure 3). Hence, based on these results, a stabilization of the $A\beta_{42}$ monomeric form and inhibition of its inclusion onto the growing oligomers, which greatly retards the overall $A\beta$ assembly process, can be rather postulated.

Protective effect of 3 on $A\beta_{42}$-induced toxicity in SH-SY5Y neuroblastoma cells. To determine whether **3** may exert any neuroprotective effect against $A\beta_{42}$-induced toxicity, a cell viability study in SH-SY5Y human neuroblastoma cells was performed using the MTT assay. Incubation of SH-SY5Y cells with 10 µM $A\beta_{42}$ resulted in a reduction of about 25% of cell viability, which can be ascribed to oligomeric species formation.[28] Non toxic concentrations of **3** and curcumin (5 and 10 µM) were then co-incubated with $A\beta_{42}$. The results depicted in Figure 4 clearly show that **3** is able to exert a dose-dependent protective effect. Indeed, while at 5 µM **3** could not prevent $A\beta_{42}$ cytotoxicity, a strong protective effect was observed when **3** was used at 10 µM. At this concentration, **3** almost completely prevented the $A\beta$-induced cell death. In the same assay, curcumin was not able to counteract $A\beta$ toxicity even at 10 µM concentration.

Antioxidant effect on H_2O_2-induced damage. To determine the potential interest of thioesters **1-3** as antioxidants, we investigated their protective effects against H_2O_2-induced oxidative damage. ROS scavenging effect was evaluated in neuroblastoma cells by using the fluorescent probe dichlorofluorescin diacetate (DCF-DA) as a specific marker for quantitative intracellular ROS formation. In comparison to untreated neuroblastoma cells (dashed line, Figure 5), the intracellular DCF-fluorescence intensity in H_2O_2-treated cells significantly increased (grey line, Figure 5). Treatment with curcumin and compounds **1-3** significantly suppressed H_2O_2-induced intracellular ROS production (Figure 5), with **2** being strongly more effective in counteracting ROS formation.
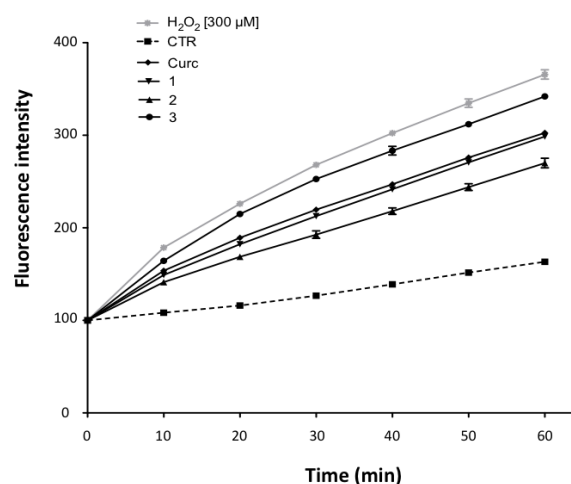
Figure 5. Compounds 1-3 reverse ROS formation-induced oxidative stress. Cells were pretreated with curcumin and compounds **1-3** (5 µM) for 24 h and then loaded with 25 µM DCF-DA for 45 min. DCF-DA was removed and cells were then exposed to 300 µM H_2O_2. Intracellular ROS levels were determined based on DCF-fluorescence by fluorescent microplate. Graph shows the intracellular fluorescence intensity of DCF $\pm$ SD in different times treatments. Fluorescence intensity for curcumin and compounds **1-3** at any time is significant with a $p < 0.001$ versus H_2O_2; Dunnett's Multiple Comparison Test.

Effect on zyxin-HIPK2-p53 signaling pathway. The pro-oxidant environment induced by $A\beta$ is well established in AD pathology, and a correlation between $A\beta$, oxidative stress and p53 conformational changes has already been suggested.[13] The mechanisms by which $A\beta$ induces zyxin and HIPK2 deregulation and the consequent p53 conformational change may therefore be related to the capability of the peptide to alter oxidative homeostasis. If this is the case, compounds with antioxidant activity should reduce $A\beta$-mediated p53 conformational change.

To substantiate this hypothesis, compounds **1-3** were further investigated in a neuroblastoma cell line to verify whether they may affect the alterations in zyxin-HIPK2-p53 pathway mediated by soluble sublethal $A\beta$ concentrations. In the used experimental conditions, $A\beta42$ (10 nM) was previously shown to modulate oxidative stress by inducing high levels of oxidative markers, such as 4-hydroxy-2-nonenal Michael-adducts and 3-nitro-
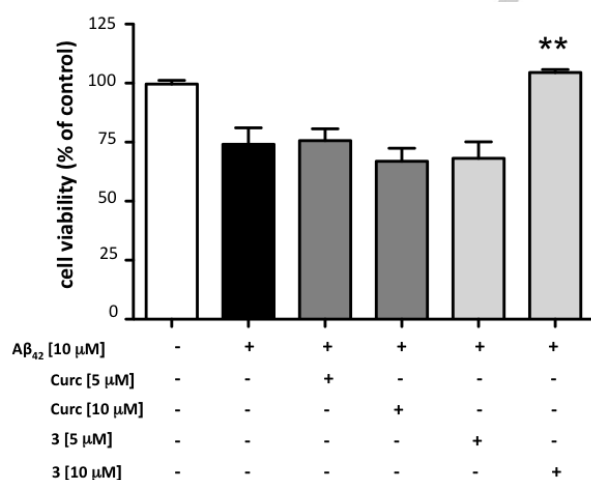

Figure 4. Effect of curcumin and compound **3** on $A\beta_{42}$ mediated cytotoxicity in neuroblastoma cells. SH-SY5Y cells were pretreated for 24 h with curcumin or **3** at 5 µM or 10 µM, and then incubated for additional 24 h with 10 µM $A\beta_{42}$. Cell viability was determined by MTT assay. Data are expressed as % of cell viability versus control. ** $p < 0.01$ versus $A\beta_{42}$; Dunnett's Multiple Comparison Test.

tyrosine and altered p53 conformation mainly due to nitration of its tyrosine residues [15-17]. However, it is worth to note that, under specific experimental conditions, and at very low concentrations (<1 nM), Aβ42 may also exert an anti-oxidative activity [18]. For further detail, in this experimental setting, we have diluted Aβ in dimethyl sulfoxide, since evidence from literature indicates that Aβ peptides, when diluted from this solvent, are quite stable and less prone to fibrilization, at near physiologic concentrations.[29]

We first characterized SH-SY5Y neuroblastoma cells in term of HIPK2 and zyxin expression and p53 conformational status. In agreement with our previous data,[14b] a sublethal concentration of Aβ$_{42}$ (10 nM) significantly reduced HIPK2 and zyxin protein levels (Figure 6a).

The conformational status of p53 was analyzed by immunoprecipitation using two conformation-specific antibodies, i.e., PAb1620 and PAb240, which discriminate folded versus unfolded p53 tertiary structure, respectively.[30] As previously verified with other cell lines, also in neuroblastoma cells Aβ$_{42}$ induced the expression of unfolded p53, as recognized by PAb240 antibody (Figure 6b).

On this basis, neuroblastoma cells were then treated with 10 nM Aβ$_{42}$ in the presence or absence of compounds 1-3 at the concentration of 5 μM. When compounds 1-3 were added to the Aβ-pretreated cells, the level of unfolded p53 was significantly lowered as shown by a lower intensity of the PAb240 positive band in comparison with that obtained when cells were treated with Aβ$_{42}$ alone. The ratio between the intensity of the bands immunoreactive to PAb240 and PAb1620, respectively, was comparable to that observed with control cells (Figure 6c), with 2 being significantly more effective. These data show that pre-treatment of neuroblastoma cells, in particular with compound 2, for which marked antioxidant properties are not accompanied by any antiaggregating activity, prevented Aβ-induced p53 conformational changes. This finding may support an involvement of the oxidative stress in Aβ function.

Loss of the p53 wild-type conformation and function induced by soluble non toxic Aβ has been shown to contribute to the accumulation of cell damage, making cells not able to activate the proper apoptotic program when exposed to noxae.[11a, 14a, 14b] In light of this evidence, we sought to study cell sensitivity to doxorubicin, a genotoxic agent able to induce apoptosis in a p53-dependent manner,[31] following treatment with 10 nM Aβ$_{42}$ in the presence or absence of 5 μM 1-3. Notably, cells treated with 1-3 and Aβ$_{42}$ showed to be more vulnerable to doxorubicin in comparison with cells treated with Aβ$_{42}$ alone. Doxorubicin induced a reduction of about 30% of cell viability in Aβ-treated cells, while the reduction of cell viability was about 50% in the presence of Aβ$_{42}$ and of each tested compound (Figure 6d). The obtained results indicate that compounds 1-3 may prevent the production of the unfolded isoform of p53 induced by Aβ, making the cells more sensitive and able to respond to an insult.
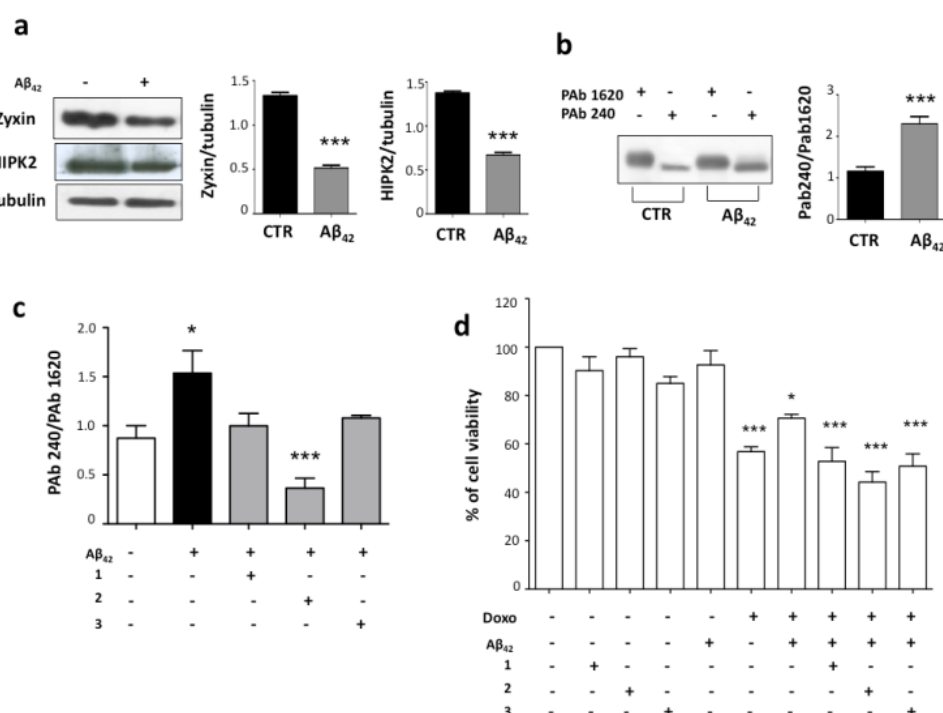

Figure 6. Compounds 1-3 positively modulate the alterations in zyxin-HIPK2-p53 pathway mediated by soluble sublethal Aβ$_{42}$. (a) Total cell extracts of SH-SY5Y cells, treated with 10 nM Aβ$_{42}$ for 48 h, were analyzed for zyxin and HIPK2 expression. Anti-tubulin was used as protein loading control. (b) SH-SY5Y cell lysates were immunoprecipitated with PAb240 or PAb1620 antibody. Immunoprecipitates were analyzed by western blot with the CM1 polyclonal anti-p53 antibody. (c) Total cell extracts of SH-SY5Y cells, incubated for 48 h with 10 nM Aβ$_{42}$ and then treated with 5 μM compounds 1-3 for 24 hours, were analyzed for p53 conformational state. Cell lysates were immunoprecipitated with PAb240 or PAb1620 antibody. Immunoprecipitates were analyzed by western blot with the CM1 polyclonal anti-p53 antibody. After densitometric analysis, data were expressed as integrated density of ratio PAb240/PAb1620 antibodies signal and represent means ± SEM of at least three different experiments. * p < 0.05, *** p < 0.001 vs Aβ treatment; Tukey's Multiple Comparison test. (d) SH-SY5Y cells were incubated with 10 nM Aβ$_{42}$ for 24 h and then treated for additional 24 h with 5 μM compounds 1-3. Cells were then resuspended in fresh medium and finally exposed to 0.5 μM doxorubicin for 24 h. Cell viability was determined by MTT assay. Data were expressed as % of cell viability versus control. * p < 0.05, *** p < 0.001 versus control; Bonferroni Multiple Comparison test.

Conclusions

The amyloidogenic pathway is thought to be crucial to the complex nature of AD. However, Aβ-centric drug programs have had limited success in AD clinical trials, so far. Yet growing evidence suggests that merely hitting Aβ production or aggregation will not be enough to undermine AD architecture, calling for a deeper understanding of Aβ functions. To this aim, we here synthesized nature-inspired compounds **1-3** to investigate the connection between Aβ and oxidative stress, with p53 emerging as a possible mediator of this functional interplay. Interestingly, the hydroxyl substituents on the aromatic moiety allowed a strategic tuning of compound's pharmacological profile. Notably, out of the three synthesized derivatives, only catechol **3** inhibited Aβ fibrils formation, underling the importance of the catechol moiety. By acting at the early stage of amyloid aggregation, **3** strongly prevented the formation of cytotoxic stable oligomeric intermediates. Conversely, although to a different extent, all hybrids were able to decrease ROS formation and inhibit Aβ-induced p53 conformational changes, with the stronger antioxidant **2**, which lacks antiaggregating properties, being significantly more effective. These findings suggest the involvement of radical species in the loss of p53 conformation and function induced by subtoxic Aβ. Most importantly, the multifunctional ligand 3, together with compounds 1 and 2, in which only the antiaggregating activity was switched off, emerge as promising pharmacologic instruments to deepen insight the molecular mechanisms potentially involved in chronic Aβ injuries.

Experimental Section

Chemistry. *General Chemical methods.* Chemical reagents were purchased from Sigma Aldrich, Fluka and Lancaster (Italy). The course of the reactions was observed by thin layer chromatography (TLC) on 0.20 mm silica gel 60 F254 plates (Merck, Germany), then visualized with an UV lamp. Nuclear magnetic resonance spectra (NMR) were recorded at 400 MHz for ^{1}H and 100 MHz for ^{13}C on Varian VXR 400 spectrometer. Chemical shifts are reported in parts per millions (ppm) relative to tetramethylsilane (TMS), and spin multiplicities are given as s (singlet), br s (broad singlet), d (doublet), t (triplet), q (quartet), or m (multiplet). Direct infusion ESI-MS mass spectra were recorded on a Waters ZQ 4000 apparatus. All final compounds **1−3** are >95% pure by HPLC analyses. The analyses were performed under reversed-phase conditions on a Phenomenex Jupiter C18 (150x4,6 mm I.D.) column, using a binary mixture (A/B) of H_2O/acetonitrile (60/40, v/v) as the mobile phase, UV detection at λ = 302 nm and a flow rate of 0.7 mL/min. The liquid chromatograph was by Jasco Corporation (Tokyo, Japan), model PU-1585 UV equipped with a 20 μL loop valve.

General procedure for the intermediates 7-9. To a solution of the appropriate *trans*-cinnamic acid **4-6** (1 equiv) in dry DMF (5 mL) were added TBDMS-Cl (2-3 equiv) and imidazole (5 equiv) under nitrogen atmosphere. After leaving the reaction at room temperature overnight, the mixture was concentrated to dryness, and the residue purified by column chromatography on silica gel to yield the desired intermediates **7-9**. Compounds **4-6** were even commercially available or synthesized as described in literature for the synthesis of *trans*-cinnamic acid trough Knoevenagel-Doebner reaction.[32]

(*E*)-3-(4-((*tert*-butyldimethylsilyl)oxy)phenyl)acrylic acid (7). Compound **7** was synthesized from **4** (500 mg, 3.04 mmol). Elution with petroleum ether/ethyl acetate (6:4) afforded **7** as a waxy solid: 466 mg (55%); ^{1}H NMR (400 MHz, CDCl$_3$) δ 7.71 (d, *J* = 16 Hz, 1H), 7.45 (d, *J* = 8.4 Hz, 2H), 6.85 (d, *J* = 8.8 Hz, 2H), 6.31 (d, *J* = 16 Hz, 1H), 0.99 (s, 9H), 0.23 (s, 6H).

(*E*)-3-(3-((*tert*-butyldimethylsilyl)oxy)phenyl)acrylic acid (8). Compound **8** was synthesized from **5** (500 mg, 3.04 mmol). Elution with petroleum ether/ethyl acetate (7:3) afforded **8** as a waxy solid: 370 mg (44%); ^{1}H NMR (400 MHz, CDCl$_3$) δ 7.72 (d, *J* = 16 Hz, 1H), 7.24 (t, *J* = 8 Hz, 1H), 7.13 (d, *J* = 7.2 Hz, 1H), 7.00 (s, 1H), 6.87 (d, *J* = 8 Hz, 1H), 6.40 (d, *J* = 16 Hz, 1H), 0.98 (s, 9H), 0.20 (s, 6H).

(*E*)-3-(3,4-bis((*tert*-butyldimethylsilyl)oxy)phenyl)acrylic acid (9). Compound **9** was synthesized from commercially available **6** (500 mg, 2.78 mmol). Elution with petroleum ether/ethyl acetate (8:2) afforded **9** as a waxy solid: 318 mg (28%); ^{1}H NMR (400 MHz, CDCl$_3$) δ 7.67 (d, *J* = 16 Hz, 1H), 7.04 (d, *J* = 6.4 Hz, 1H), 7.03 (s, 1H), 6.82 (d, *J* = 8.4 Hz, 1H), 6.22 (d, *J* = 15.6 Hz, 1H), 0.96 (s, 18H), 0.19 (s, 12H).

General procedure for the intermediates 10-12. To an ice-cooled solution of the appropriate acid (**7-9**) (1 equiv) in dry CH$_2$Cl$_2$ (4 mL) was added DCC (1.1 equiv), and DMAP (cat.). The reaction mixture was stirred for 10', followed by addition of 2-propene-1-thiol (3 equiv). Stirring was then continued at room temperature overnight, and the reaction worked up by filtration and evaporation. The crude was purified by chromatography on silica gel.

***S*-allyl (*E*)-3-(4-((*tert*-butyldimethylsilyl)oxy)phenyl)prop-2-enethioate (10).** Compound **10** was synthesized from **7** (160 mg, 0.575 mmol). Elution with petroleum ether/ethyl acetate (9.8:0.2) afforded **10** as a waxy solid: 100 mg (52%); ^{1}H NMR (400 MHz, CDCl$_3$) δ 7.57 (d, *J* = 15.6 Hz, 1H), 7.43 (d, *J* = 8.8 Hz, 2H), 6.84 (d, *J* = 8.4 Hz, 2H), 6.59 (d, *J* = 15.6 Hz, 1H), 5.88-5.83 (m, 1H), 5.28 (d, *J* = 16.8 Hz, 1H), 5.13 (d, *J* = 10 Hz, 1H), 3.66 (d, *J* = 6.8, 2H), 0.98 (s, 9H), 0.22 (s, 6H).

***S*-allyl (*E*)-3-(3-((*tert*-butyldimethylsilyl)oxy)phenyl)prop-2-enethioate (11).** Compound **11** was synthesized from **8** (370 mg, 1.33 mmol). Elution with petroleum ether/ethyl acetate (9.8:0.2) afforded **11** as a waxy solid: 260 mg (58%); ^{1}H NMR (400 MHz, CDCl$_3$) δ 7.57 (d, *J* = 15.6 Hz, 1H), 7.15 (t, *J* = 8 Hz, 1H), 7.08 (d, *J* = 8.8 Hz, 1H), 7.02 (s, 1H), 6.89 (d, *J* = 8.4 Hz, 1H), 6.66 (d, *J* = 15.6 Hz, 1H), 5.88-5.83 (m, 1H), 5.28 (d, *J* = 16 Hz, 1H), 5.13 (d, *J* = 10 Hz 1H), 3.66 (d, *J* = 6.4 Hz, 2H), 0.97 (s, 9H), 0.20 (s, 6H).

***S*-allyl (*E*)-3-(3,4-bis((*tert*-butyldimethylsilyl)oxy)phenyl)prop-2-enethioate (12).** Compound **12** was synthesized from **9** (200 mg, 0.500 mmol). Elution with petroleum ether/ethyl acetate (9.5:0.5) afforded **12** as a waxy solid: 160 mg (70%); ^{1}H NMR (400 MHz, CDCl$_3$) δ 7.49 (d, *J* = 16 Hz, 1H), 7.00 (d, *J* = 7.2 Hz, 1H), 6.80 (d, *J* = 8 Hz, 1H), 6.72 (s, 1H), 6.50 (d, *J* = 15.6 Hz, 1H), 5.76-5.65 (m, 1H), 5.25 (d, *J* = 16.8 Hz, 1H), 5.09 (d, *J* = 10.1 Hz, 1H), 3.56 (d, *J* = 6.8 Hz, 2H), 0.97 (s, 9H), 0.96 (s, 9H), 0.19 (s, 6H), 0.18 (s, 6H).

General procedure for the synthesis of 1-3. To a solution of the appropriate organosilane intermediate **10-12** (1 equiv) in THF (5 mL) was added TBAF (4 equiv) and stirring was continued at room temperature. After 20-30 min, the reaction was quenched by addition of saturated aqueous NH$_4$Cl solution; the aqueous phase was extracted with EtOAc (3 x 10 mL), and the combined organic layers were dried over Na$_2$SO$_4$. Following evaporation of the solvent, the residue was purified by column chromatography on silica gel.

S-allyl (E)-3-(4-hydroxyphenyl)prop-2-enethioate (1). Compound **1** was synthesized from **10** (100 mg, 0.299 mmol). Elution with petroleum ether/ethyl acetate (7:3) afforded **1** as a waxy solid: 30 mg (46%); ^{1}H NMR (400 MHz, CDCl$_3$) δ 7.56 (d, J = 16 Hz, 1H), 7.42 (d, J = 8.4 Hz, 2H), 6.84 (d, J = 8.4 Hz, 2H), 6.58 (d, J = 15.6 Hz, 1H), 5.88-5.81 (m, 1H), 5.29-5.25 (d, J = 16.8 Hz, 1H), 5.13-5.10 (d, J = 10.8 Hz, 1H), 3.65 (d, J = 7.2 Hz, 2H). ^{13}C-NMR (CDCl$_3$, 100 MHz) δ 189.97, 158.23, 140.83, 133.05, 130.44, 126.66, 122.29, 118.02, 116.03, 31.80. MS [ESI$^+$] m/z 243 [M+Na]$^+$.

S-allyl (E)-3-(3-hydroxyphenyl)prop-2-enethioate (2). Compound **2** was synthesized from **11** (210 mg, 0.63 mmol). Elution with CH$_2$Cl$_2$/MeOH (9.7:0.3) afforded **2** as a waxy solid: 110 mg (79%); ^{1}H NMR (400 MHz, CDCl$_3$) δ 7.54 (d, J = 16 Hz, 1H), 7.24 (t, J = 7.2 Hz, 1H), 7.08 (d, J = 7.6 Hz, 1H), 7.02 (s, 1H), 6.90 (d, J = 7.6 Hz, 1H), 6.58 (d, J = 15.6 Hz, 1H), 6.09 (br s, 1H), 5.88-5.81 (m, 1H), 5.28 (d, J = 16.8 Hz, 1H), 5.13 (d, J = 10 Hz, 1H), 3.65 (d, J = 6.4 Hz, 2H). ^{13}C-NMR (CDCl$_3$, 100 MHz) δ 190.33, 156.20, 140.85, 135.43, 132.75, 130.22, 124.89, 121.12, 118.31, 118.05, 114.91, 31.94. MS [ESI$^-$] m/z 219 [M-H]$^-$.

S-allyl (E)-3-(3,4-dihydroxyphenyl)prop-2-enethioate (3). Compound **3** was synthesized from **12** (160 mg, 0.344 mmol). Elution with petroleum ether/ethyl acetate (5:5) afforded **3** as a waxy solid: 50 mg (62%); ^{1}H NMR (400 MHz, CD$_3$OD) δ 7.54 (d, J = 15.6 Hz, 1H), 7.10 (s, 1H), 7.02 (d, J = 7.6 Hz, 1H), 6.84 (d, J = 7.6 Hz, 1H), 6.63 (d, J = 15.2 Hz, 1H), 5.94-5.87 (m, 1H), 5.31 (d, J = 16.8 Hz, 1H), 5.14 (d, J = 10 Hz, 1H), 3.68 (d, J = 6.4 Hz, 2H). ^{13}C-NMR (CD$_3$OD, 100 MHz) δ 189.34, 148.56, 145.47, 141.37, 133.43, 125.91, 122.14, 120.93, 116.56, 115.18, 113.93, 30.94. MS [ESI$^+$] m/z 259 [M+Na]$^+$.

Aβ$_{42}$ self-aggregation: sample preparation. 1,1,1,3,3,3-Hexafluoro-2-propanol (HFIP) pre-treated Aβ$_{42}$ samples (Bachem AG, Switzerland) were resolubilized with a CH$_3$CN/Na$_2$CO$_3$/NaOH (48.4/48.4/3.2) mixture to have a stable stock solution ([Aβ$_{42}$] = 500 μM).[33] Tested inhibitors were dissolved in methanol and diluted in the assay buffer. Experiments were performed by incubating the peptide diluted in 10 mM phosphate buffer (pH = 8.0) containing 10 mM NaCl, at 30 °C (Thermomixer Comfort, Eppendorf, Italy) for 24 h (final Aβ concentration = 50 μM) with and without inhibitor.

Inhibition of Aβ$_{42}$ self-aggregation: ThT assay. Inhibition studies were performed by incubating Aβ$_{42}$ samples in the assay conditions reported above, with and without tested inhibitors. Inhibitors were first screened at 50 μM in a 1/1 ratio with Aβ$_{42}$. To quantify amyloid fibril formation, the ThT fluorescence method was used.[20b, 34] After incubation, samples were diluted to a final volume of 2.0 mL with 50 mM glycine-NaOH buffer (pH = 8.5) containing 1.5 μM ThT. A 300-seconds-time scan of fluorescence intensity was carried out ($λ_{exc}$ = 446 nm; $λ_{em}$ = 490 nm), and values at plateau were averaged after subtracting the background fluorescence of 1.5 μM ThT solution. Blanks containing inhibitor and ThT were also prepared and evaluated to account for quenching and fluorescence properties. The fluorescence intensities were compared and the % inhibition was calculated. For compound **3**, the IC$_{50}$ value was also determined. To this aim four increasing concentrations were tested. IC$_{50}$ value was obtained from the % inhibition vs log[inhibitor] plot.

Inhibition of Aβ$_{42}$ self-aggregation by 3: Flow injection-ESI-MS method. Inhibition studies were performed by incubating Aβ$_{42}$ samples in the assay conditions reported above, with and without the tested inhibitor **3** or curcumin. At t0 and t24h, aliquots with and without inhibitor were analyzed by flow injection-ESI-IT-MS. LC-MS analyses were performed as described in Fiori et al.[24] Briefly, the Aβ$_{42}$ samples were analyzed by 10-μL loop injection after previous addition of reserpine as internal standard. ESI-IT-MS analyses were performed on a Jasco PU-1585

Liquid Chromatograph (Jasco, Tokyo, Japan) interfaced with LCQ Duo Mass Spectrometer (Thermo Finnigan, San Jose, CA, USA) equipped with an electrospray ionization (ESI) source operating with an ion trap analyzer. The mobile phase consisted of 0.1% (v/v) formic acid in acetonitrile/water 30/70. ESI system employed a 4.5 kV spray voltage and a capillary temperature of 200°C. Mass spectra were operated in positive polarity, in the scan range of 200-2000 m/z and at the scan rate of 3 microscans/sec. Single ion monitoring (SIM) chromatograms for the quantitative analysis were reconstructed at the base peaks corresponding to the differently charged amyloid monomer ions (Native, N) and oxidized ions (Ox). The ratio between the total monomer area and the IS area was used for Aβ$_{42}$ monomer determination. The Area$_{total\ monomer}$/Area$_{IS}$ ratio at t0 is considered as 100% of the monomer content. The results were expressed as means ± SD of three independent experiments and a p value < 0.05 was considered statistically significant (Dunnett's Multiple Comparison Test).

Reagents for cellular experiments. All culture media, supplements and Foetal Bovine Serum (FBS) were obtained from Euroclone (Life Science Division, Milan, Italy). Electrophoresis reagents were obtained from Bio-Rad (Hercules, CA, USA). All other reagents were of the highest grade available and were purchased from Sigma Chemical Co. (St. Louis, MO, USA) unless otherwise indicated. Aβ$_{42}$ was solubilised in dimethyl sulfoxide (DMSO) at the concentration of 100 μM and frozen in stock aliquots that were diluted at the final concentration of 10 nM prior to use. For each experimental setting, one aliquot of the stock was thawed out and diluted at the final concentration of 10 nM to minimize peptide damage due to repeated freeze and thaw. The Aβ$_{42}$ concentration was chosen following dose response experiments (data not shown) where maximal modulation of p53 structure and its transcriptional activity[35] was obtained at 10 nM. All the experiments performed with Aβ$_{42}$ were made in 1% of serum. H$_2$O$_2$ was diluted to working concentration (1 mM) in phosphate buffer saline (PBS) at the moment of use. Mouse monoclonal anti α-tubulin was purchased from Sigma-Aldrich (St. Louis, MO, USA). Host specific peroxidase conjugated IgG secondary antibodies were obtained from Pierce (Rockford, IL, USA).

Cell cultures. Human neuroblastoma SH-SY5Y cells from European Collection of Cell Cultures (ECACC No. 94030304) were cultured in medium with equal amount of Eagle's minimum essential medium and Nutrient Mixture Ham's F-12, supplemented with 10% foetal bovine serum, glutamine (2mM), penicillin/streptomycin, non-essential aminoacids at 37 °C in 5%CO2/95% air.

Cell viability. The mitochondrial dehydrogenase activity that reduces 3-(4,5-dimethylthiazol-2-yl)-2,5-diphenyl-tetrazolium bromide (MTT, Sigma, St Louis, MO, USA) was used to determine cellular viability, in a quantitative colorimetric assay. At day 0 SH-SY5Y cells were plated at a density of 2x10^4 viable cells per well in 96-well plates. After treatment, according to the experimental setting, cells were exposed to an MTT solution in PBS (1 mg/mL). Following 4 h incubation with MTT and treatment with SDS for 24 h, cell viability reduction was quantified by using a BIO-RAD microplate reader (Model 550; Hercules, CA, USA).

Measurement of intracellular ROS. DCF-DA (Sigma Aldrich) was used to estimate intracellular ROS. Briefly, cells (2 × 10^4 cells/well) were pretreated with reference curcumin and compounds **1-3** (5 μM) for 24 h and then loaded with 25 μM DCF-DA at 37°C for 45 min. DCF-DA was removed after centrifuge and cells were resuspended in PBS and then exposed to 300 μM H$_2$O$_2$. The results were visualized using Synergy HT microplate reader (BioTek) with excitation and emission wavelengths of 485 nm and 530 nm, respectively.

Immunodetection of zyxin and HIPK2. Cell monolayers were washed twice with ice cold PBS, lysed on the tissue culture dish by addition of ice-cold lysis buffer (50 mM Tris/HCl pH 7.4, 150mM NaCl, 50 mM EDTA, 0.2 mM 4-(2-aminoethyl) benzenesulfonyl fluoride hydrochloride (AEBSF), 20 µg/ml leupeptin, 25 µg/ml aprotinin, 0,5 µg/ml pepstatin A and 1% Triton X-100) and an aliquot was used for protein analysis with the Pierce Bicinchoninic Acid kit, for protein quantification. Cell lysates were diluited in sample buffer (62.5 mM Tris/HCl pH 6.8, 2% SDS, 10% glycerol, 50 mM dithiothreitol, 0.1% Bromophenol blue) and subjected to Western blot analysis. Proteins were subjected to SDS-PAGE (8%) and then transferred onto PVDF membrane 0,45µm (Immobilion, Millipore Corp, Bedford, MA,USA). The membrane was blocked for 1 h with 5% non-fat dry milk in Tris-buffered saline containing 0.1% Tween 20 (TBST). Membranes were immunoblotted with the rabbit anti human zyxin or HIPK2 polyclonal antibody (at 1:1000 dilution in 5% non fat dry milk, from Cell Signaling Technology, EuroClone, Milan, Italy). The detection was carried out by incubation with horseradish peroxidase conjugated goat anti-rabbit IgG (1:5000 dilution in 5% non fat dry milk, from Pierce, Rockford,IL, USA) for 1 h. The blots were then washed extensively and the proteins of interest were visualized using an enhanced chemiluminescent method (Pierce, Rockford, IL, USA). Tubulin was also performed as a normal control of proteins.

p53 conformational immunoprecipitation. p53 conformational state was analyzed by immunoprecipitation as detailed previously.[10a] Briefly, cells were lysed in immunoprecipitation buffer (10 mM Tris, pH 7.6; 140 mM NaCl; and 0.5% NP40 including protease inhibitors); 100 µg of total cell extracts were used for immunoprecipitation experiments performed in a volume of 500 µl with 1 µg of the conformation-specific antibodies PAb1620 (wild-type specific) or PAb240 (mutant specific) (Neomarkers, CA, USA). Immunocomplexes were separated by 10% SDS-PAGE and immunoblotting was performed with rabbit anti-p53 antibody (FL393) (Santa Cruz, CA, USA). Immunoreactivity was detected with the ECL-chemiluminescence reaction kit (Amersham, Little Chalfont, UK).

Densitometry and statistics. All the experiments, unless specified, were performed at least three times. Following acquisition of the Western blot image through an AGFA scanner and analysis by means of the Image 1.47 program (Wayne Rasband, NIH, Research Services Branch, NIMH, Bethesda, MD, USA), the relative densities of the bands were analyzed as described previously.[36] The data were analyzed by analysis of variance (ANOVA) followed when significant by an appropriate post hoc comparison test as indicated in figure legend. The reported data are expressed as means ± SD of at least three independent experiments. A p value < 0.05 was considered statistically significant.

[1] a) D. J. Selkoe, *Behav Brain Res* **2008**, *192*, 106-113; b) J. Laurén, D. A. Gimbel, H. B. Nygaard, J. W. Gilbert, S. M. Strittmatter, *Nature* **2009**, *457*, 1128-1132.

[2] a) E. Karran, M. Mercken, B. De Strooper, *Nat Rev Drug Discov* **2011**, *10*, 698-712; b) K. Herrup, *Nat Neurosci* **2015**, *18*, 794-799.

[3] a) E. Mura, F. Pistoia, M. Sara, S. Sacco, A. Carolei, S. Govoni, *Curr Pharm Des* **2014**, *20*, 4121-4139; b) L. M. Ittner, J. Götz, *Nat Rev Neurosci* **2011**, *12*, 65-72; c) Z. Esposito, L. Belli, S. Toniolo, G. Sancesario, C. Bianconi, A. Martorana, *CNS Neurosci Ther* **2013**, *19*, 549-555.

[4] a) E. Viayna, I. Sola, M. Bartolini, A. De Simone, C. Tapia-Rojas, F. G. Serrano, R. Sabaté, J. Juárez-Jiménez, B. Pérez, F. J. Luque, V. Andrisano, M. V. Clos, N. C. Inestrosa, D. Muñoz-Torrero, *J Med Chem* **2014**, *57*, 2549-2567; b) E. Nepovimova, E. Uliassi, J. Korabecny, L. E. Peña-Altamira, S. Samez, A. Pesaresi, G. E. Garcia, M. Bartolini, V. Andrisano, C. Bergamini, R. Fato, D. Lamba, M. Roberti, K. Kuca, B. Monti, M. L. Bolognesi, *J Med Chem* **2014**, *57*, 8576-8589; c) M. Rosini, E. Simoni, M. Bartolini, E. Soriano, J. Marco-Contelles, V. Andrisano, B. Monti, M. Windisch, B. Hutter-Paier, D. W. McClymont, I. R. Mellor, M. L. Bolognesi, *ChemMedChem* **2013**, *8*, 1276-1281; d) M. Rosini, V. Andrisano, M. Bartolini, M. L. Bolognesi, P. Hrelia, A. Minarini, A. Tarozzi, C. Melchiorre, *J Med Chem* **2005**, *48*, 360-363; e) M. Rosini, E. Simoni, M. Bartolini, A. Cavalli, L. Ceccarini, N. Pascu, D. W. McClymont, A. Tarozzi, M. L. Bolognesi, A. Minarini, V. Tumiatti, V. Andrisano, I. R. Mellor, C. Melchiorre, *J Med Chem* **2008**, *51*, 4381-4384.

[5] a) A. Cavalli, M. L. Bolognesi, A. Minarini, M. Rosini, V. Tumiatti, M. Recanatini, C. Melchiorre, *J Med Chem* **2008**, *51*, 347-372; b) M. Rosini, *Future Med Chem* **2014**, *6*, 485-487; c) A. Anighoro, J. Bajorath, G. Rastelli, *J Med Chem* **2014**, *57*, 7874-7887.

[6] M. Rosini, E. Simoni, A. Milelli, A. Minarini, C. Melchiorre, *J Med Chem* **2014**, *57*, 2821-2831.

[7] M. Coma, F. X. Guix, G. Ill-Raga, I. Uribesalgo, F. Alameda, M. A. Valverde, F. J. Muñoz, *Neurobiol Aging* **2008**, *29*, 969-980.

[8] A. M. Swomley, S. Förster, J. T. Keeney, J. Triplett, Z. Zhang, R. Sultana, D. A. Butterfield, *Biochim Biophys Acta* **2014**, *1842*, 1248-1257.

[9] a) S. Salvioli, M. Capri, L. Bucci, C. Lanni, M. Racchi, D. Uberti, M. Memo, D. Mari, S. Govoni, C. Franceschi, *Cancer Immunol Immunother* **2009**, *58*, 1909-1917; b) W. Chatoo, M. Abdouh, G. Bernier, *Antioxid Redox Signal* **2011**, *15*, 1729-1737; c) A. Salminen, K. Kaarniranta, *Cell Signal* **2011**, *23*, 747-752.

[10] a) D. Uberti, C. Lanni, T. Carsana, S. Francisconi, C. Missale, M. Racchi, S. Govoni, M. Memo, *Neurobiol Aging* **2006**, *27*, 1193-1201; b) C. Lanni, M. Racchi, G. Mazzini, A. Ranzenigo, R. Polotti, E. Sinforiani, L. Olivari, M. Barcikowska, M. Styczynska, J. Kuznicki, A. Szybinska, S. Govoni, M. Memo, D. Uberti, *Mol Psychiatry* **2008**, *13*, 641-647; c) X. Zhou, J. Jia, *Neurosci Lett* **2010**, *468*, 320-325.

[11] a) D. Uberti, T. Carsana, E. Bernardi, L. Rodella, P. Grigolato, C. Lanni, M. Racchi, S. Govoni, M. Memo, *J Cell Sci* **2002**, *115*, 3131-3138; b) Y. Yang, D. S. Geldmacher, K. Herrup, *J Neurosci* **2001**, *21*, 2661-2668.

[12] P. Hainaut, J. Milner, *Cancer Res* **1993**, *53*, 4469-4473.

[13] C. Lanni, M. Racchi, M. Memo, S. Govoni, D. Uberti, *Free Radic Biol Med* **2012**, *52*, 1727-1733.

[14] a) C. Lanni, L. Nardinocchi, R. Puca, S. Stanga, D. Uberti, M. Memo, S. Govoni, G. D'Orazi, M. Racchi, *PLoS One* **2010**, *5*, e10171; b) C. Lanni, D. Necchi, A. Pinto, E. Buoso, L. Buizza, M. Memo, D. Uberti, S. Govoni, M. Racchi, *J Neurochem* **2013**, *125*, 790-799; c) E. Mura, S. Zappettini, S. Preda, F. Biundo, C. Lanni, M. Grilli, A. Cavallero, G. Olivero, A. Salamone, S. Govoni, M. Marchi, *PLoS One* **2012**, *7*, e29661.

[15] J. Crone, C. Glas, K. Schultheiss, J. Moehlenbrink, E. Krieghoff-Henning, T. G. Hofmann, *Cancer Res* **2011**, *71*, 2350-2359.

[16] S. Rizzo, H. Waldmann, *Chem Rev* **2014**, *114*, 4621-4639.

[17] a) C. B. Pocernich, M. L. Lange, R. Sultana, D. A. Butterfield, *Current Alzheimer research* **2011**, *8*, 452-469; b) M. Stefani, S. Rigacci, *Int J Mol Sci* **2013**, *14*, 12411-12457.

[18] S. Kim, H. G. Lee, S. A. Park, J. K. Kundu, Y. S. Keum, Y. N. Cha, H. K. Na, Y. J. Surh, *PLoS One* **2014**, *9*, e85984.

[19] a) G. Gerenu, K. Liu, J. E. Chojnacki, J. M. Saathoff, P. Martinez-Martin, G. Perry, X. Zhu, H. G. Lee, S. Zhang, *ACS Chem Neurosci* **2015**; b) E. Simoni, C. Bergamini, R. Fato, A. Tarozzi, S. Bains, R. Motterlini, A. Cavalli, M. L. Bolognesi, A. Minarini, P. Hrelia, G. Lenaz, M. Rosini, C. Melchiorre, *J Med Chem* **2010**, *53*, 7264-7268.

[20] a) M. Groenning, L. Olsen, M. van de Weert, J. M. Flink, S. Frokjaer, F. S. Jørgensen, *J Struct Biol* **2007**, *158*, 358-369; b) H. Naiki, K. Higuchi, M. Hosokawa, T. Takeda, *Anal Biochem* **1989**, *177*, 244-249.

[21]   A. Minarini, A. Milelli, V. Tumiatti, M. Rosini, E. Simoni, M. L. Bolognesi, V. Andrisano, M. Bartolini, E. Motori, C. Angeloni, S. Hrelia, *Neuropharmacology* **2012**, *62*, 997-1003.

[22]   A. F. McKoy, J. Chen, T. Schupbach, M. H. Hecht, *J Biol Chem* **2012**, *287*, 38992-39000.

[23]   M. Bartolini, M. Naldi, J. Fiori, F. Valle, F. Biscarini, D. V. Nicolau, V. Andrisano, *Anal Biochem* **2011**, *414*, 215-225.

[24]   J. Fiori, M. Naldi, M. Bartolini, V. Andrisano, *Electrophoresis* **2012**, *33*, 3380-3386.

[25]   a) C. G. Glabe, R. Kayed, *Neurology* **2006**, *66*, S74-78; b) M. P. Lambert, A. K. Barlow, B. A. Chromy, C. Edwards, R. Freed, M. Liosatos, T. E. Morgan, I. Rozovsky, B. Trommer, K. L. Viola, P. Wals, C. Zhang, C. E. Finch, G. A. Krafft, W. L. Klein, *Proc Natl Acad Sci U S A* **1998**, *95*, 6448-6453; c) D. M. Walsh, I. Klyubin, J. V. Fadeeva, W. K. Cullen, R. Anwyl, M. S. Wolfe, M. J. Rowan, D. J. Selkoe, *Nature* **2002**, *416*, 535-539.

[26]   S. C. Forester, J. D. Lambert, *Mol Nutr Food Res* **2011**, *55*, 844-854.

[27]   L. Hou, I. Kang, R. E. Marchant, M. G. Zagorski, *J Biol Chem* **2002**, *277*, 40173-40176.

[28]   S. Sabella, M. Quaglia, C. Lanni, M. Racchi, S. Govoni, G. Caccialanza, A. Calligaro, V. Bellotti, E. De Lorenzi, *Electrophoresis* **2004**, *25*, 3186-3194.

[29]   H. LeVine, *Anal Biochem* **2004**, *335*, 81-90.

[30]   C. Méplan, M. J. Richard, P. Hainaut, *Biochem Pharmacol* **2000**, *59*, 25-33.

[31]   a) K. Hayakawa, M. Hasegawa, M. Kawashima, Y. Nakamura, M. Matsuura, H. Toda, N. Mitsuhashi, H. Niibe, *Oncol Rep* **2000**, *7*, 267-270; b) E. Lorenzo, C. Ruiz-Ruiz, A. J. Quesada, G. Hernández, A. Rodríguez, A. López-Rivas, J. M. Redondo, *J Biol Chem* **2002**, *277*, 10883-10892; c) S. Wang, E. A. Konorev, S. Kotamraju, J. Joseph, S. Kalivendi, B. Kalyanaraman, *J Biol Chem* **2004**, *279*, 25535-25543.

[32]   C. N. Xia, H. B. Li, F. Liu, W. X. Hu, *Bioorg Med Chem Lett* **2008**, *18*, 6553-6557.

[33]   M. Bartolini, C. Bertucci, M. L. Bolognesi, A. Cavalli, C. Melchiorre, V. Andrisano, *Chembiochem* **2007**, *8*, 2152-2161.

[34]   H. LeVine, *Protein Sci* **1993**, *2*, 404-410.

[35]   D. Uberti, G. Cenini, L. Olivari, G. Ferrari-Toninelli, E. Porrello, C. Cecchi, A. Pensalfini, A. Pensafini, G. Liguri, S. Govoni, M. Racchi, M. Maurizio, *J Neurochem* **2007**, *103*, 322-333.

[36]   C. Lanni, M. Mazzucchelli, E. Porrello, S. Govoni, M. Racchi, *Eur J Biochem* **2004**, *271*, 3068-3075.

FULL PAPER

Shedding light on amyloid-β: nature-inspired multifunctional ligands **1-3** allowed to explore the molecular mechanisms potentially engaged in chronic Aβ injuries. This study supports the involvement of oxidative stress in Aβ function, with p53 emerging as a potential mediator of their functional interplay.
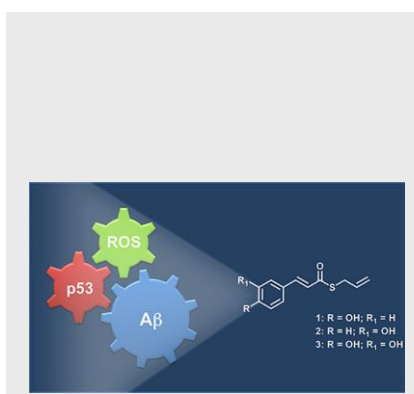
Elena Simoni, Melania M. Serafini, Manuela Bartolini, Roberta Caporaso, Antonella Pinto, Daniela Necchi, Jessica Fiori, Vincenza Andrisano, Anna Minarini, Cristina Lanni,* and Michela Rosini*

Nature-inspired multifunctional ligands: focusing on amyloid-based molecular mechanisms of Alzheimer's disease